

Soft Diffusion Actor-Critic: Efficient Online Reinforcement Learning for Diffusion Policy

Haitong Ma¹, Tianyi Chen², Kai Wang², Na Li^{*1}, and Bo Dai^{*2}

¹*School of Engineering and Applied Sciences, Harvard University*

²*School of Computational Science and Engineering, Georgia Institute of Technology*[†]

Abstract

Diffusion policies have achieved superior performance in imitation learning and offline reinforcement learning (RL) due to their rich expressiveness. However, the vanilla diffusion training procedure requires samples from target distribution, which is impossible in online RL since we cannot sample from the optimal policy, making training diffusion policies highly non-trivial in online RL. Backpropagating policy gradient through the diffusion process incurs huge computational costs and instability, thus being expensive and impractical. To enable efficient diffusion policy training for online RL, we propose Soft Diffusion Actor-Critic (SDAC), exploiting the viewpoint of diffusion models as noise-perturbed energy-based models. The proposed SDAC relies solely on the state-action value function as the energy functions to train diffusion policies, bypassing sampling from the optimal policy while maintaining lightweight computations. We conducted comprehensive comparisons on MuJoCo benchmarks. The empirical results show that SDAC outperforms all recent diffusion-policy online RLs on most tasks, and improves more than 120% over soft actor-critic on complex locomotion tasks such as Humanoid and Ant.

1 Introduction

Huge successes of diffusion-based generative models have been witnessed recently [Sohl-Dickstein et al. \(2015\)](#); [Song & Ermon \(2019\)](#); [Ho et al. \(2020\)](#). With a dual interpretation of latent variable models and energy-based models (EBMs), diffusion models achieved superior expressiveness and multimodality in representing complex probability distributions, demonstrating unprecedented performance in image and video generation [Ramesh et al. \(2021\)](#); [Saharia et al. \(2022\)](#). The superior expressiveness and multimodality naturally benefit the policies in sequential decision-making problems. In fact, diffusion policy has been introduced in imitation learning and offline reinforcement learning (RL), where expert datasets are presented. Due to the flexibility of diffusion models, it improved significantly over previous deterministic or unimodal policies on manipulation [Chi et al. \(2023\)](#); [Ke et al. \(2024\)](#); [Scheikl et al. \(2024\)](#) and locomotion tasks [Huang et al. \(2024\)](#).

Meanwhile, online RL has long been seeking expressive policy families. Specifically, [Haarnoja et al. \(2017\)](#) showed that the optimal stochastic policy of online RL lies in energy-based models (EBMs), *i.e.*, unnormalized probabilistic models. EBMs are inherently flexible and multimodal due to their unnormalized nature. However, sampling and evaluation of EBMs are notoriously difficult due to their intractable likelihood [Song & Kingma \(2021\)](#). A variety of parametrized probabilistic models have been introduced for efficient sampling and learning but with the payoff of approximation error. For example, a representative

*Equal supervision.

[†]Emails: Haitong Ma (haitongma@g.harvard.edu), Tianyi Chen (tchen667@gatech.edu), Kai Wang (kwang692@gatech.edu), Na Li (nali@seas.harvard.edu), Bo Dai (bodai@cc.gatech.edu)

maximum entropy RL algorithm is the well-known soft actor-critic (SAC, Haarnoja et al., 2018a) that has been the state-of-the-art in online RL. However, SAC restricts the policy space to Gaussian distributions, thereby losing the inherent expressiveness and multimodality of energy-based models (EBMs).

Diffusion models have been shown to be closely related to energy-based models (EBMs), as they can be interpreted as EBMs with multi-level noise perturbations Song & Ermon (2019); Shribak et al. (2024). The multi-level noise perturbations significantly improve the sampling quality, making diffusion policies the perfect fit to represent the energy-based policies. However, it is highly non-trivial to train diffusion policies in the context of online RL. The vanilla procedure to train diffusion models requires sampling from target data distribution, which refers to the optimal policy in online RL. However, we can not sample from the optimal policies in online RL directly. Several studies have explored alternative approaches to overcome this limitation. For example, Psenka et al. (2023); Jain et al. (2024) directly match the score functions with derivatives of the learned Q -functions and sample with Langevin dynamics. Yang et al. (2023) maintain a large number of action particles and fit it with diffusion models. Wang et al. (2024) backpropagate the policy gradient thorough the whole reverse diffusion process. Ding et al. (2024a) approximate the policy optimization by maximum likelihood estimation reweighted by the Q -function. All these methods still encounter various challenges due to inaccurate approximations and/or huge memory and computation costs, limiting the true potential of diffusion policies in online RL.

To handle these challenges, we propose the Soft Diffusion Actor-Critic (SDAC), an efficient algorithm to train diffusion policies in online RL without sampling from optimal policies. Specifically,

- Developing upon the viewpoint of diffusion models as noise-perturbed EBMs, we first propose the reverse sampling score matching (RSSM), an algorithm to train diffusion models with only access to the energy function (*i.e.*, unnormalized density) while *bypassing sampling from the data distribution*.
- We then show that the RSSM enables efficient diffusion policy training when fit into online RL, which leads to a practical implementation named Soft Diffusion Actor-Critic (SDAC). No specific sampling protocol or recurrent gradient backpropagation is needed during the policy learning stage. We also address practical issues such as exploration and numerical stability.
- We demonstrated empirical results, showing that the proposed SDAC outperforms all recent diffusion policy online RL baselines in most OpenAI Gym MuJoCo benchmarks. Moreover, the performance is increased by **more than 120% over SAC** on complex locomotion tasks such as MuJoCo Humanoid and Ant, demonstrating the true potential of diffusion policy in online RL.

2 Preliminaries

We introduce the necessary preliminaries in this section. First, we introduce Markov decision process and maximum entropy reinforcement learning as our policy learning framework, followed by a recap of diffusion models.

2.1 Maximum Entropy Reinforcement Learning

Markov Decision Processes (MDPs). We consider Markov decision process (Puterman, 2014) specified by a tuple $\mathcal{M} = (\mathcal{S}, \mathcal{A}, r, P, \mu_0, \gamma)$, where \mathcal{S} is the state space, \mathcal{A} is the action space, $r : \mathcal{S} \times \mathcal{A} \rightarrow \mathbb{R}$ is a reward function, $P(\cdot|s, a) : \mathcal{S} \times \mathcal{A} \rightarrow \Delta(\mathcal{S})$ is the transition operator with $\Delta(\mathcal{S})$ as the family of distributions over \mathcal{S} , $\mu_0 \in \Delta(\mathcal{S})$ is the initial distribution and $\gamma \in (0, 1)$ is the discount factor.

Maximum entropy RL. We follow the maximum entropy RL to learn our diffusion policies Haarnoja et al.

(2017). We consider the following entropy-regularized expected return as the policy learning objective,

$$\arg \max_{\pi} J(\pi) := \mathbb{E}_{\pi} \left[\sum_{\tau=0}^{\infty} \gamma^{\tau} (r(\mathbf{s}_{\tau}, \mathbf{a}_{\tau}) + \lambda \mathcal{H}(\pi(\cdot | \mathbf{s}_{\tau}))) \right] \quad (1)$$

where $\mathcal{H}(\pi(\cdot | \mathbf{s})) = \mathbb{E}_{\mathbf{a} \sim \pi(\cdot | \mathbf{s})} [-\log \pi(\mathbf{a} | \mathbf{s})]$ is the entropy, λ is a regularization coefficient for the entropy. The soft policy iteration algorithm Haarnoja et al. (2017, 2018a) is proposed to solve the optimal max-entropy policy. Soft policy iteration algorithm iteratively conducts soft policy evaluation and soft policy improvement, where soft policy evaluation updates the soft Q -function by repeatedly applying soft Bellman update operator \mathcal{T}^{π} to current value function $Q : \mathcal{S} \times \mathcal{A} \rightarrow \mathbb{R}$, *i.e.*,

$$\mathcal{T}^{\pi} Q(\mathbf{s}_{\tau}, \mathbf{a}_{\tau}) = r(\mathbf{s}_{\tau}, \mathbf{a}_{\tau}) + \gamma \mathbb{E}_{\mathbf{s}_{\tau+1} \sim P} [V(\mathbf{s}_{\tau+1})] \quad (2)$$

where $V(\mathbf{s}_{\tau}) = \mathbb{E}_{\mathbf{a}_{\tau} \sim \pi} [Q(\mathbf{s}_{\tau}, \mathbf{a}_{\tau}) - \lambda \log \pi(\mathbf{a}_{\tau} | \mathbf{s}_{\tau})]$ Haarnoja et al. (2018a). Then in the soft policy improvement stage, the policy is updated to fit the target policy

$$\pi_{\text{target}}(\mathbf{a} | \mathbf{s}) \propto \exp \left(\frac{1}{\lambda} Q^{\pi_{\text{old}}}(\mathbf{s}, \mathbf{a}) \right) \quad (3)$$

where π_{old} is the current policy and $Q^{\pi_{\text{old}}}$ is the converged result of (2) with $\mathcal{T}^{\pi_{\text{old}}}$.

Soft Actor-Critic. Although we have closed-form policy (3), it is a *unnormalized* distribution, often referred to as an *energy-based* policy since the unnormalized density is called energy function in literature, which is notoriously difficult to sample from and learn. To enable efficient computation, a natural idea is to approximate the energy-based policies (3) with a parametrized distribution. A representative algorithm is the well-known soft actor-critic (SAC), which restricts the policy to be a parametrized Gaussian, *i.e.*, $\pi_{\theta}(a | s) = \mathcal{N}(\mu_{\theta_1}(s), \sigma_{\theta_2}^2(s))$ and updates the parameters $\theta = [\theta_1, \theta_2]$ by optimizing the KL -divergence to the target policy $D_{KL}(\pi_{\theta} || \pi_{\text{target}})$ Haarnoja et al. (2018a) via policy gradient with parametrization trick, *i.e.*,

$$J_{\text{SAC}}^{\pi}(\theta) = \mathbb{E}_{\mathbf{s} \sim \mathcal{D}, \mathbf{a} \sim \pi_{\theta}} [\lambda \log \pi_{\theta}(\mathbf{a} | \mathbf{s}) - Q^{\pi_{\text{old}}}(\mathbf{s}, \mathbf{a})].$$

The Gaussian approximation loses the inherent expressiveness and multimodality of energy-based policies, thus limiting the performance of maximum entropy RL algorithms. This limitation motivates the pursuit of more expressive policy structures to further enhance performance.

2.2 Denoising Diffusion Probabilistic Models

Denoising diffusion probabilistic models (DDPMs, Sohl-Dickstein et al., 2015; Song & Ermon, 2019; Ho et al., 2020) are powerful tools to represent and generate complex probability distributions. *Given data samples from the data distribution p_0* , DDPMs are composed of a forward diffusion process that gradually perturbs the data distribution $\mathbf{x}_0 \sim p_0$ to a noise distribution $\mathbf{x}_T \sim p_T$, and a reverse diffusion process that reconstructs data distribution p_0 from noise distribution p_T . The forward corruption kernel is usually Gaussian with a variance schedule β_1, \dots, β_T , resulting in the forward trajectories with joint distribution

$$q_{0:T}(\mathbf{x}_{0:T}) = p_0(\mathbf{x}_0) \prod_{t=1}^T q_{t|t-1}(\mathbf{x}_t | \mathbf{x}_{t-1}) \quad \text{where} \\ q_{t|t-1}(\mathbf{x}_t | \mathbf{x}_{t-1}) := \mathcal{N}(\mathbf{x}_t; \sqrt{1 - \beta_t} \mathbf{x}_{t-1}, \beta_t \mathbf{I}) \quad (4)$$

where \mathbf{x}_t is random variable at t step, and p, q are probability distributions¹. The backward process recovers the data distribution from a noise distribution p_T with a series of reverse kernels $p_{t-1|t}(\mathbf{x}_{t-1} | \mathbf{x}_t)$. The reverse kernels are usually intractable so we parameterize it with neural networks denoted as $p_{\theta; t-1|t}(\mathbf{x}_{t-1} | \mathbf{x}_t)$, resulting in a joint distribution of the reverse process,

$$p_{\theta}(\mathbf{x}_{0:T}) = p_T(\mathbf{x}_T) \prod_{t=1}^T p_{\theta; t-1|t}(\mathbf{x}_{t-1} | \mathbf{x}_t)$$

¹We use p and q interchangeably as density function in this paper. Generally, p represents intractable distributions (like the t -step marginal $p_t(\mathbf{x}_t)$), and q represents tractable distributions such as the Gaussian corruption $q_{t|t-1}(\mathbf{x}_t | \mathbf{x}_{t-1})$.

Considering all $(\mathbf{x}_1, \dots, \mathbf{x}_T)$ as the latent variables, we can solve the parameters θ via optimizing the evidence lower bound (ELBO) over \mathbf{x}_0 ,

$$\text{ELBO}(\theta) = \mathbb{E}_{\mathbf{x}_0 \sim p_0} \mathbb{E}_{\mathbf{x}_{1:T} \sim q} \left[\log \frac{p_\theta(\mathbf{x}_{0:T})}{q(\mathbf{x}_{1:T}|\mathbf{x}_0)} \right].$$

After fixing $p_{\theta;t-1|t}$ to be Gaussian and reparametrizing $p_{\theta;t-1|t}$ with a score network² $s_\theta(\mathbf{x}_t; t)$, maximizing the ELBO is equivalent to minimizing a collection of denoising score matching loss over multiple noise levels indexed by t Vincent (2011); Ho et al. (2020),

$$\mathcal{L}_{\text{DSM}}(\theta) := \frac{1}{T} \sum_{t=0}^T (1 - \bar{\alpha}_t) \mathbb{E}_{\substack{\mathbf{x}_0 \sim p_0 \\ \mathbf{x}_t \sim q_{t|0}}} \left[\|s_\theta(\mathbf{x}_t; t) - \nabla \log q_{t|0}(\mathbf{x}_t|\mathbf{x}_0)\|^2 \right] \quad (5)$$

where $q_{t|0}(\mathbf{a}_t|\mathbf{a}_0) := \mathcal{N}(\mathbf{a}_t; \sqrt{\bar{\alpha}_t}\mathbf{a}_0, (1 - \bar{\alpha}_t)\mathbf{I})$ and $\bar{\alpha}_t = \prod_{l=1}^t (1 - \beta_l)$. After learning the s_θ by minimizing (5), we can draw sample via the reverse diffusion process by iteratively conducting

$$\mathbf{x}_{t-1} = \frac{1}{\sqrt{\bar{\alpha}_t}} (\mathbf{x}_t + \beta_t s_\theta(\mathbf{x}_t, t)) + \frac{1 - \bar{\alpha}_{t-1}}{1 - \bar{\alpha}_t} \beta_t \mathbf{z}_t \quad (6)$$

for $t = T, T-1, \dots, 1$ and $\mathbf{z}_t \sim \mathcal{N}(0, \mathbf{I})$.

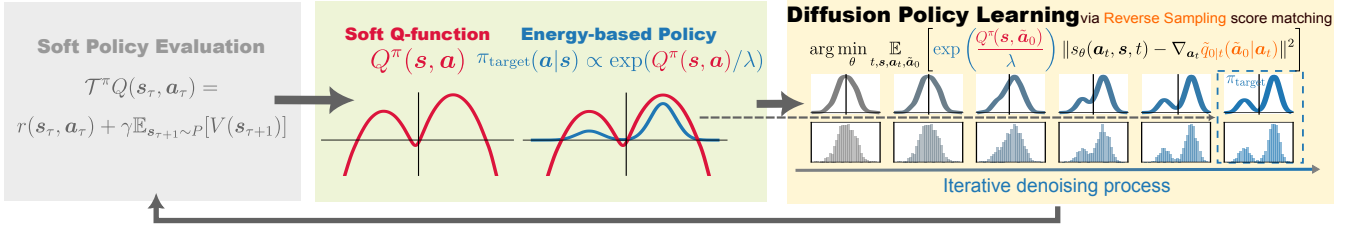


Figure 1: Demonstration of the proposed Soft Diffusion Actor-Critic (SDAC) algorithm. We leverage diffusion policy to represent the energy-based policy in maximum entropy RL. The diffusion policy is trained via reverse sampling score matching, an algorithm that does not sample from the target energy-based policy and only depends on the Q -functions, enabling efficient online RL for diffusion policy.

3 Diffusion Policy Learning in Online RL

In this section, we first present the connection of energy-based models and diffusion models, justifying the expressiveness of diffusion policy, and identify the difficulties in online training of diffusion policy. We then introduce the reverse sampling score matching (RSSM) to make the training of diffusion policy possible with *only* access to the energy function in online RL.

3.1 Diffusion Models as Noise-Perturbed Energy-Based Models

We first revisit the energy-based view of diffusion models, *i.e.*, *diffusion models are noise-perturbed EBMs* Shribak et al. (2024), to justify that the diffusion policy can efficiently represent the energy-based π_{target} . Given \mathbf{s} , consider perturbing action samples $\mathbf{a}_0 \sim \pi_{\text{target}}(\cdot|\mathbf{s})$ with corruption kernel $q_{t|0}(\mathbf{a}_t|\mathbf{a}_0) = \mathcal{N}(\mathbf{a}_t; \sqrt{\bar{\alpha}_t}\mathbf{a}_0, (1 - \bar{\alpha}_t)\mathbf{I})$, which results in the noisy-perturbed policy $\tilde{\pi}_t(\cdot|\mathbf{s})$ with

$$\tilde{\pi}_t(\mathbf{a}_t|\mathbf{s}) = \int q_{t|0}(\mathbf{a}_t|\mathbf{a}_0) \pi_{\text{target}}(\mathbf{a}_0|\mathbf{s}) d\mathbf{a}_0$$

for noise schedule index $t = 1, 2, \dots, T$.

Proposition 3.1 (Diffusion models as noise-perturbed EBMs). *The score network $s_\theta(\mathbf{a}_t; \mathbf{s}, t)$ in (5) matches noise-perturbed score functions, $\nabla_{\mathbf{a}_t} \log \tilde{\pi}_t(\mathbf{a}_t|\mathbf{s})$, where state \mathbf{s} is added to inputs of score network*

²Some paper reparameterize it as the noise prediction network ϵ_θ , but they are the same in essence since $\nabla_{\mathbf{x}_t} \log q_{t|0}(\mathbf{x}_t|\mathbf{x}_0) = -\frac{\mathbf{x}_t - \sqrt{\bar{\alpha}_t}\mathbf{x}_0}{1 - \bar{\alpha}_t} = -\frac{\epsilon}{\sqrt{1 - \bar{\alpha}_t}}$ for Gaussian noise ϵ .

$s_\theta(\mathbf{a}_t; \mathbf{s}, t)$ to handle conditional distributions, $p_0(\cdot)$ in (5) refers to $\pi_{\text{target}}(\cdot|\mathbf{s})$ in the policy learning setting.

Proof. This can be shown by checking the noise-perturbed score function $\nabla_{\mathbf{a}_t} \log \tilde{\pi}_t(\mathbf{a}_t|\mathbf{s}_t)$, i.e.,

$$\begin{aligned} & \nabla_{\mathbf{a}_t} \log \tilde{\pi}_t(\mathbf{a}_t|\mathbf{s}_t) \\ &= \frac{\nabla_{\mathbf{a}_t} \tilde{\pi}_t(\mathbf{a}_t|\mathbf{s})}{\tilde{\pi}_t(\mathbf{a}_t|\mathbf{s})} = \frac{\nabla_{\mathbf{a}_t} \int q_{t|0}(\mathbf{a}_t|\mathbf{a}_0) \pi_{\text{target}}(\mathbf{a}_0|\mathbf{s}) d\mathbf{a}_0}{\tilde{\pi}_t(\mathbf{a}_t|\mathbf{s})} \\ &= \int \nabla_{\mathbf{a}_t} \log q_{t|0}(\mathbf{a}_t|\mathbf{a}_0) \underbrace{\frac{q_{t|0}(\mathbf{a}_t|\mathbf{a}_0) \pi_{\text{target}}(\mathbf{a}_0|\mathbf{s})}{\tilde{\pi}_t(\mathbf{a}_t|\mathbf{s})}}_{p_{0|t}(\mathbf{a}_0|\mathbf{a}_t, \mathbf{s})} d\mathbf{a}_0 \end{aligned} \quad (7)$$

We match the noise-perturbed score function via the score network $s_\theta(\mathbf{a}_t; \mathbf{s}, t)$ via optimizing the expectation of square error over $\mathbf{a}_t \sim \tilde{\pi}_t(\cdot|\mathbf{s})$,

$$\begin{aligned} & \mathbb{E}_{\mathbf{a}_t \sim \tilde{\pi}_t} \left\| s_\theta(\mathbf{a}_t; \mathbf{s}, t) - \int \nabla_{\mathbf{a}_t} \log q_{t|0}(\mathbf{a}_t|\mathbf{a}_0) p_{0|t}(\mathbf{a}_0|\mathbf{a}_t, \mathbf{s}) d\mathbf{a}_0 \right\|^2 \\ &= \mathbb{E}_{\substack{\mathbf{a}_0 \sim \pi_{\text{target}} \\ \mathbf{a}_t \sim q_{t|0}}} \left[\left\| s_\theta(\mathbf{a}_t; \mathbf{s}, t) - \nabla_{\mathbf{a}_t} \log q_{t|0}(\mathbf{a}_t|\mathbf{a}_0) \right\|^2 \right] + \text{constant} \end{aligned} \quad (8)$$

The detailed derivations of (8) are deferred to Appendix B.1. We can see that (8) is equivalent to the t -th term in DDPM loss (5), which concludes the proof of Proposition 3.1. \square

Furthermore, as the noise schedule β_t gets close to zero when t goes from T to 1 in the reverse process (6), the noise-perturbed EBMs gradually resemble the original energy-based policies π_{target} . Adding adaptive levels of noise perturbations encourages explorations on the energy landscape, which significantly improves the sampling quality and makes diffusion models the key breakthrough in EBMs Song & Ermon (2019).

Difficulties to train diffusion model in online RL setup. By the connection between EBMs and diffusion models, we justify the expressiveness of diffusion policy for maximum entropy RL. However, training diffusion policy is highly non-trivial in online RL because of two major challenges:

- **Sampling challenge:** the vanilla diffusion training with denoising score matching (5) requires samples from the target policy π_{target} , but we cannot access π_{target} directly in online RL since we only know the energy function, i.e., the Q -functions.
- **Computational challenge:** another possible solution is to backpropagate policy gradient thorough the whole reverse diffusion process (6). However, this recursive gradient propagation not only incurs huge computational and memory cost, but also suffers from gradient vanishing or exploding, making diffusion policy learning expensive and unstable.

These challenges hinder the performance of diffusion-based policies in online RL.

3.2 Learning Noise-perturbed Score Functions via Reverse Sampling Score Matching

In this section, we develop our core contribution, reverse sampling score matching (RSSM), an efficient diffusion policy learning algorithm that eliminates the aforementioned difficulties. Following the energy-based viewpoint in Proposition 3.1, we propose the following theorem,

Theorem 3.2 (Reverse sampling score matching (RSSM)). *Define $\tilde{p}_t(\cdot|\mathbf{s})$ as a sampling distribution whose support contains the support of $\tilde{\pi}_t(\cdot|\mathbf{s})$ given \mathbf{s} . Then we can learn the score network $s_\theta(\mathbf{a}_t; \mathbf{s}, t)$ to match*

with the score function of noise-perturbed policy $\nabla_{\mathbf{a}_t} \log \tilde{\pi}_t(\mathbf{a}_t | \mathbf{s})$ via minimizing

$$\mathbb{E}_{\substack{\mathbf{a}_t \sim \tilde{p}_t \\ \tilde{\mathbf{a}}_0 \sim \tilde{q}_{0|t}}} \left[\exp(Q(\mathbf{s}, \tilde{\mathbf{a}}_0) / \lambda) \left\| s_\theta(\mathbf{a}_t; \mathbf{s}, t) - \nabla \tilde{q}_{0|t}(\tilde{\mathbf{a}}_0 | \mathbf{a}_t) \right\|^2 \right] \quad (9)$$

where we abbreviate $Q^{\pi_{\text{old}}}$ with Q for simplicity and $\tilde{q}_{0|t}$ is the **reverse sampling** distribution defined as

$$\tilde{q}_{0|t}(\tilde{\mathbf{a}}_0 | \mathbf{a}_t) := \mathcal{N} \left(\mathbf{a}_0; \frac{1}{\sqrt{\bar{\alpha}_t}} \mathbf{a}_t, \frac{1 - \bar{\alpha}_t}{\bar{\alpha}_t} \mathbf{I} \right) \quad (10)$$

which means $\tilde{\mathbf{a}}_0 = \frac{1}{\sqrt{\bar{\alpha}_t}} \mathbf{a}_t - \sqrt{\frac{1 - \bar{\alpha}_t}{\bar{\alpha}_t}} \boldsymbol{\epsilon}$ for $\boldsymbol{\epsilon} \sim \mathcal{N}(0, \mathbf{I})$.

The name *reverse sampling* score matching comes from that we first sample $\mathbf{a}_t \sim \tilde{p}_t$ then sample $\tilde{\mathbf{a}}_0 \sim \tilde{q}_{0|t}$, thus bypassing the sampling issues and not increasing computational cost. We show a sketch proof here, the full derivations can be found in Appendix B.2.

Proof. The derivations consists of two major steps, reformulating the noise-perturbed score function and applying the reverse sampling trick.

Reformatting the noise-perturbed score function. First, we slightly reformat derivations of the noise-perturbed score function in Proposition 3.1 starting from (7),

$$\begin{aligned} \nabla_{\mathbf{a}_t} \log \tilde{\pi}_t(\mathbf{a}_t | \mathbf{s}) &= \int \nabla_{\mathbf{a}_t} \log q_{t|0}(\mathbf{a}_t | \mathbf{a}_0) \frac{q_{t|0}(\mathbf{a}_t | \mathbf{a}_0) \pi_{\text{target}}(\mathbf{a}_0 | \mathbf{s})}{\tilde{\pi}_t(\mathbf{a}_t | \mathbf{s})} d\mathbf{a}_0 \\ &= \frac{\int \nabla_{\mathbf{a}_t} \log q_{t|0}(\mathbf{a}_t | \mathbf{a}_0) q_{t|0}(\mathbf{a}_t | \mathbf{a}_0) \exp(Q(\mathbf{s}, \mathbf{a}_0) / \lambda) d\mathbf{a}_0}{Z(\mathbf{a}_t; \mathbf{s})} \end{aligned} \quad (11)$$

where $Z(\mathbf{a}_t; \mathbf{s}) := \tilde{\pi}_t(\mathbf{a}_t | \mathbf{s}) \int \exp(Q(\mathbf{s}, \mathbf{a}_0) / \lambda) d\mathbf{a}_0 = \int q_{t|0}(\mathbf{a}_t | \mathbf{a}_0) \exp(Q(\mathbf{s}, \mathbf{a}_0) / \lambda) d\mathbf{a}_0$. Equation (11) is obtained by substituting the energy function into π_{target} . With (11), the square error given \mathbf{a}_t satisfies

$$\|s_\theta(\mathbf{a}_t; \mathbf{s}, t) - \nabla_{\mathbf{a}_t} \log \tilde{\pi}_t(\mathbf{a}_t | \mathbf{s})\|^2 = \frac{1}{Z(\mathbf{a}_t; \mathbf{s})} \int q_{t|0}(\mathbf{a}_t | \mathbf{a}_0) \exp(Q(\mathbf{s}, \mathbf{a}_0) / \lambda) l_\theta(\mathbf{a}_0, \mathbf{a}_t; \mathbf{s}) d\mathbf{a}_0 \quad (12)$$

where $l_\theta(\mathbf{a}_0, \mathbf{a}_t; \mathbf{s}) = \|s_\theta(\mathbf{a}_t; \mathbf{s}, t) - \nabla_{\mathbf{a}_t} \log q_{t|0}(\mathbf{a}_t | \mathbf{a}_0)\|^2$. Then we integrate the square error over a custom measure $g(\mathbf{a}_t; \mathbf{s}) := Z(\mathbf{a}_t; \mathbf{s}) \tilde{p}_t(\mathbf{a}_t | \mathbf{s})$ to compensate the $Z(\mathbf{a}_t; \mathbf{s})$ and get to,

$$\iint \tilde{p}_t(\mathbf{a}_t | \mathbf{s}) q_{t|0}(\mathbf{a}_t | \mathbf{a}_0) \exp(Q(\mathbf{s}, \mathbf{a}_0) / \lambda) l_\theta(\mathbf{a}_0, \mathbf{a}_t; \mathbf{s}) d\mathbf{a}_0 d\mathbf{a}_t \quad (13)$$

A more rigorous derivation is deferred to Appendix B.2.

Reverse sampling trick. The loss function in (13) is still not tractable. To handle this, we introduce the *reverse sampling trick*, i.e., replacing $q_{t|0}$ with a reverse sampling distribution $\tilde{q}_{0|t}$ that satisfies

$$\begin{aligned} \tilde{q}_{0|t}(\mathbf{a}_0 | \mathbf{a}_t) &= \mathcal{N} \left(\mathbf{a}_0; \frac{1}{\sqrt{\bar{\alpha}_t}} \mathbf{a}_t, \frac{1 - \bar{\alpha}_t}{\bar{\alpha}_t} \mathbf{I} \right) \\ &\propto q_{t|0}(\mathbf{a}_t | \mathbf{a}_0) = \mathcal{N}(\mathbf{a}_t; \sqrt{\bar{\alpha}_t} \mathbf{a}_0, (1 - \bar{\alpha}_t) \mathbf{I}), \end{aligned} \quad (14)$$

and their score functions match $\nabla_{\mathbf{a}_t} \log q_{t|0}(\mathbf{a}_t | \mathbf{a}_0) = \nabla_{\mathbf{a}_t} \log \tilde{q}_{0|t}(\mathbf{a}_0 | \mathbf{a}_t) = -\frac{\mathbf{a}_t - \sqrt{\bar{\alpha}_t} \mathbf{a}_0}{1 - \bar{\alpha}_t}$. Then we can replace $q_{t|0}$ with $\tilde{q}_{0|t}$ in (13) to get a tractable loss function,

$$\iint \tilde{p}_t(\mathbf{a}_t | \mathbf{s}) \tilde{q}_{0|t}(\tilde{\mathbf{a}}_0 | \mathbf{a}_t) \exp(Q(\mathbf{s}, \tilde{\mathbf{a}}_0) / \lambda) \tilde{l}_\theta(\mathbf{a}_0, \mathbf{a}_t; \mathbf{s}) d\tilde{\mathbf{a}}_0 d\mathbf{a}_t \quad (15)$$

where $\tilde{l}_\theta(\mathbf{a}_0, \mathbf{a}_t; \mathbf{s}) = \|s_\theta(\mathbf{a}_t; \mathbf{s}, t) - \nabla_{\mathbf{a}_t} \log \tilde{q}_{0|t}(\tilde{\mathbf{a}}_0 | \mathbf{a}_t)\|^2$. In this way, we can first sample $\mathbf{a}_t \sim \tilde{p}_t$ and then sample $\tilde{\mathbf{a}}_0 \sim \tilde{q}_{0|t}$ to enable tractable loss computation. By further algebraic operations, we can derive the loss function in (9) from (15). The detailed derivation can be found in Appendix B.2. \square

We can see that with Theorem 3.2, the loss function (9) solves both the sampling and computational difficulties mentioned previously. First, we avoid sampling from target policy π_{target} , and the sampling distribution \tilde{p}_t is some distributions we can choose. Second, we have similar computation with denoising score matching (5), avoiding extra computational cost induced by diffusion policy learning.

Remark 3.3 (Broader applications of RSSM.). We emphasize that although we develop RSSM for online RL problems, the RSSM has its own merit and can be applied to any probabilistic modeling problems with known energy functions. We also show a toy example in Section 5.1 where we use RSSM to train a toy diffusion model to generate samples from a Gaussian mixture distribution.

Remark 3.4 (Pitfalls of Langevin dynamics in online RL.). Some might question that if we already know the energy function, why not compute the gradient as the score functions and use the Langevin dynamics Parisi (1981) to sample from policy (3). The reasons are two-fold, i) the gradient of learned Q -function might not match the true score function; ii) Langevin dynamics suffers from the slow mixing problem (Song & Ermon, 2019, shown in Section 5.1) even with true score functions. Both pitfalls result in bad performance and motivate the necessity of diffusion policies with known energy functions.

3.3 Practical Diffusion Policy Learning Loss

The direct impact of Theorem 3.2 is a diffusion policy learning loss that can be sampled and computed efficiently in online RL. Specifically, summing over all timestep t and state \mathbf{s} in Equation (9), we derive the diffusion policy learning loss with RSSM:

$$\mathcal{L}^\pi(\theta; Q, \lambda) := \frac{1}{T} \sum_{t=1}^T \mathbb{E}_{\mathbf{s}, \mathbf{a}_t, \tilde{\mathbf{a}}_0} \left[\exp\left(\frac{Q(\mathbf{s}, \tilde{\mathbf{a}}_0)}{\lambda}\right) \left\| s_\theta(\mathbf{a}_t, \mathbf{s}, t) - \nabla_{\mathbf{a}_t} \tilde{q}_{0|t}(\tilde{\mathbf{a}}_0 | \mathbf{a}_t) \right\|^2 \right] \quad (16)$$

with

$$\tilde{\mathbf{a}}_0 = \frac{1}{\sqrt{\bar{\alpha}_t}} \mathbf{a}_t - \sqrt{\frac{1 - \bar{\alpha}_t}{\bar{\alpha}_t}} \boldsymbol{\epsilon}, \quad \boldsymbol{\epsilon} \sim \mathcal{N}(0, \mathbf{I}) \quad (17)$$

and \mathbf{s} sampled from the replay buffer, \mathbf{a}_t sampled from $\tilde{p}_t(\cdot | \mathbf{s})$.

Obviously, such sampling protocol in (16) and (17) bypasses sampling from the target optimal policy, therefore, can be easily implemented. Meanwhile, the obtained loss avoids recursive gradient backpropagation, largely reducing computation complexity of policy gradient. These benefits perfectly echo the difficulties of sampling and computations in applying vanilla diffusion model training to online RL, enabling efficient diffusion policy learning.

4 Soft Diffusion Actor Critic

In this section, we propose the Soft Diffusion Actor-Critic (SDAC), a practical maximum entropy RL algorithm leveraging RSSM to train diffusion policy to represent energy-based policies. We first address several practical issues such as sampling scheme and exploration-exploitation tradeoff and then present the overall algorithm.

4.1 Practical Issues of Diffusion Policy Training

Reverse sampling distribution selection. In the theoretical derivation, we did not specify which sampling distribution \tilde{p}_t to use. In the online RL setting, we need to query the Q function when we calculate the diffusion policy loss (16). As $Q^\pi(\mathbf{s}, \mathbf{a})$ gets more accurate, it is better to have the sampled $\tilde{\mathbf{a}}_0$ being closer to the target policy (3), *i.e.*, sample $\tilde{\mathbf{a}}_0$ such that $Q^\pi(\mathbf{s}, \tilde{\mathbf{a}}_0)$ is of high values. In practice, we use samples generated from the reverse diffusion process in soft policy evaluation step to achieve better performance.

Exploration and exploitation trade-off is key to online RL performance. Haarnoja et al. (2018b) proposed to automatically tune the regularization parameter λ to fit a target entropy proportional to the action space dimension, but it is impractical for diffusion policy since the entropy is intractable for EBMs.

Current diffusion online RLs either estimated entropy with Gaussian mixture model Wang et al. (2024), or mixed sampling with uniform samples Ding et al. (2024a) to encourage exploration. However, these operations significantly increase the computation cost and slow down the training, which is unnecessary. In our practical implementations, we simplified the exploration design by adding additive Gaussian noise with level λ . Therefore, the parameter λ controls the policy randomness in two ways, the energy function scale and the additional Gaussian noise. The λ is also auto-tuned to track a target noise level λ_{target} .

Numerical stability. The loss function re-weights the common denoising score matching loss (18) by exponential of Q -function. In practice, the exponential of large Q functions will cause the loss to explode. Moreover, the scale of the Q function might vary with different rewards or tasks. To improve numerical stability, we normalized the Q function, *i.e.*, subtracting the mean and dividing by the standard deviation. The normalization operation does not conflict with our theoretical derivation, subtracting mean values is scaling the loss, and the standard deviation can be regarded as part of the regularization hyperparameter λ .

4.2 Practical Algorithm

Combining all the discussions above, we present the practical algorithm in Algorithm 1 and also in Figure 1.

Algorithm 1 Soft Diffusion Actor-Critic

Require: Diffusion noise schedule $\beta_t, \bar{\alpha}_t$ for $t \in \{1, 2, \dots, T\}$, reverse sampling distribution $\tilde{\pi}_t$, MDP \mathcal{M} , initial policy parameters θ_0 , initial entropy coefficient λ_0 , replay buffer $\mathcal{D} = \emptyset$, learning rate β , target entropy coefficient λ_{target}

- 1: **for** epoch $e = 1, 2, \dots$ **do**
- 2: *# Sampling and experience replay.*
- 3: Interact with \mathcal{M} using policy $\epsilon_{\theta_{e-1}}$ thorough algorithm update replay buffer \mathcal{D} .
- 4: Sample a minibatch of $(\mathbf{s}, \mathbf{a}, r, \mathbf{s}')$ from \mathcal{D} .
- 5: *# Soft policy evaluation.*
- 6: Sample \mathbf{a}' via reverse diffusion process (6) with $\epsilon_{\theta_{e-1}}$.
- 7: Update Q_e with soft policy evaluation (2).
- 8: *# Soft policy improvement for diffusion policies.*
- 9: Randomly sample t and $\mathbf{a}_t \sim \tilde{\pi}_t(\cdot|\mathbf{s})$.
- 10: *Reverse sampling:* Sample $\tilde{\mathbf{a}}_0$ with (17).
- 11: Compute $Q_e(\mathbf{s}, \tilde{\mathbf{a}}_0)$ and normalize as $\bar{Q}_e(\mathbf{s}, \tilde{\mathbf{a}}_0)$.
- 12: Update θ_e with loss $\mathcal{L}^\pi(\theta_{e-1}; \bar{Q}_e, \lambda_{e-1})$ in (16).
- 13: Update entropy coefficient $\lambda_e \leftarrow \lambda_{e-1} - \beta(\lambda_e - \lambda_{\text{target}})$.
- 14: **end for**

Efficiency and performance compared to other diffusion policies for online RL. We say the proposed SDAC algorithm in Algorithm 1 is efficient because of similar computation and memory cost with denoising score matching (5) while maintaining performance and bypassing the sampling issues, which is more efficient compared to recent diffusion policies for online RL.

Recent works on diffusion policy online RLs can be categorized into these families: **i) Langevin-based sampling.** With the known energy functions in (3), Psenka et al. (2023); Jain et al. (2024) directly differentiated it to get the score function and use Langevin dynamics to sample from (3). The computation is lightweight since no noise perturbation is involved (thus not diffusion policies in essence). However, the empirical performance is not good due to pitfalls mentioned in Remark 3.4. **ii) Reverse diffusion as policy parametrizations.** The reverse process (6) can also be directly regarded as a complex parametrization of θ . Wang et al. (2024) backpropagate policy gradients through the reverse

diffusion process, resulting in huge computation costs. Ding et al. (2024a) approximate the policy learning as a maximum likelihood estimation for the reverse process, which incurs approximation errors and can not handle negative Q -values. **iii) Others.** Yang et al. (2023) maintained particles to approximate the policy distribution and fit it with the diffusion model. Ren et al. (2024) combined the reverse process MDP with MDP in RL and conducted policy optimizations. They all induce huge memory and computation costs, thus being impractical and unnecessary. More general related works can be found in Appendix A.

5 Experimental Results

This section presents the experimental results. We first use a toy example, generating a 2D Gaussian mixture, to verify the effectiveness of the proposed RSSM as diffusion model training. Then we show the empirical results of the proposed SDAC algorithm evaluated with OpenAI Gym MuJoCo tasks.

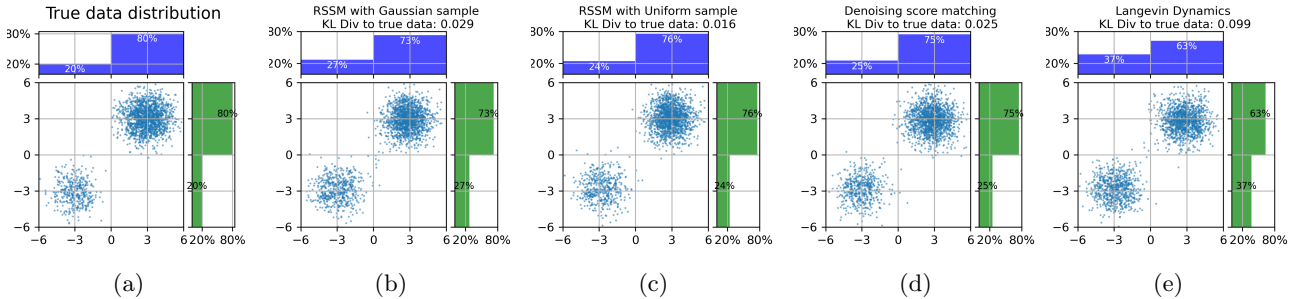


Figure 2: The scatter plots of generating 2D Gaussian mixture, the histograms show the partition on each axis. Figure 2(a) shows the true data samples with mixing coefficients $[0.8, 0.2]$. Fig. 2(b), 2(c), 2(d) show that both the proposed RSSM (with two sample schemes) and denoising score matching can approximately recover the true data distribution. Figure 2(e) shows the slow mixing of Langevin dynamics that the mixing coefficients can not be correctly recovered.

Table 1: Performance on OpenAI Gym MuJoCo environments. The numbers show the best mean returns and standard deviations over 200k iterations and 5 random seeds.

		HALFCHEETAH	REACHER	HUMANOID	PUSHER	INVERTEDPENDULUM
Classic Model-Free RL	PPO	4852 \pm 732	-8.69 \pm 11.50	952 \pm 259	-25.52 \pm 2.60	1000 \pm 0
	TD3	8149 \pm 688	-3.10 \pm 0.07	5816 \pm 358	-25.07 \pm 1.01	1000 \pm 0
	SAC	8981 \pm 370	-65.35 \pm 56.42	2858 \pm 2637	-31.22 \pm 0.26	1000 \pm 0
Diffusion Policy RL	QSM	10740 \pm 444	-4.16 \pm 0.28	5652 \pm 435	-80.78 \pm 2.20	1000 \pm 0
	DIPO	9063 \pm 654	-3.29 \pm 0.03	4880 \pm 1072	-32.89 \pm 0.34	1000 \pm 0
	DACER	11203 \pm 246	-3.31 \pm 0.07	2755 \pm 3599	-30.82 \pm 0.13	801 \pm 446
	QVPO	7321 \pm 1087	-30.59 \pm 16.57	421 \pm 75	-129.06 \pm 0.96	1000 \pm 0
	DPPO	1173 \pm 392	-6.62 \pm 1.70	484 \pm 64	-89.31 \pm 17.32	1000 \pm 0
	SDAC (ours)	11924 \pm 609	-3.14 \pm 0.10	6959 \pm 460	-30.43 \pm 0.37	1000 \pm 0
		ANT	HOPPER	SWIMMER	WALKER2D	INVERTED2PENDULUM
Classic Model-Free RL	PPO	3442 \pm 851	3227 \pm 164	84.5 \pm 12.4	4114 \pm 806	9358 \pm 1
	TD3	3733 \pm 1336	1934 \pm 1079	71.9 \pm 15.3	2476 \pm 1357	9360 \pm 0
	SAC	2500 \pm 767	3197 \pm 294	63.5 \pm 10.2	3233 \pm 871	9359 \pm 1
Diffusion Policy RL	QSM	938 \pm 164	2804 \pm 466	57.0 \pm 7.7	2523 \pm 872	2186 \pm 234
	DIPO	965 \pm 9	1191 \pm 770	46.7 \pm 2.9	1961 \pm 1509	9352 \pm 3
	DACER	4301 \pm 524	3212 \pm 86	103.0 \pm 45.8	3194 \pm 1822	6289 \pm 3977
	QVPO	718 \pm 336	2873 \pm 607	53.4 \pm 5.0	2337 \pm 1215	7603 \pm 3910
	DPPO	60 \pm 15	2175 \pm 556	106.1 \pm 6.5	1130 \pm 686	9346 \pm 4
	SDAC (ours)	5683 \pm 138	3275 \pm 55	79.3 \pm 52.5	4365 \pm 266	9360 \pm 0

5.1 Toy Example

We first show a toy example of generating a 2D Gaussian mixture dataset to verify the effectiveness of the proposed RSSM loss in training diffusion models as generative models. The Gaussian mixture model is composed of two modes whose mean values are $[3, 3]$ and $[-3, -3]$ and mixing coefficients are 0.8 and 0.2 shown in Figure 2(a). The detailed training setup can be found in Appendix C.1.

We compare diffusion models trained with three loss functions: **a.** proposed RSSM loss (9) with $\tilde{p}_t = \mathcal{N}(0, 4\mathbf{I})$ for all t in Figure 2(b). **b.** proposed RSSM loss (9) with uniform sampling distribution $\tilde{p}_t = \text{Unif}([-6, 6])$ for all t in 2(c). Both two RSSM algorithms have access to the true energy function but cannot sample directly from the true data. **c.** the commonly used denoising score matching loss (5) in Figure 2(d), which has access to the true data. We also show the naive Langevin dynamics Parisi (1981) samples as a reference in Figure 2(e), which has access to the true score function.

Empirical results showed that both two diffusion models trained by RSSM and the one trained by vanilla denoising score matching can approximately recover both two modes and the mixing coefficients, which verifies the effectiveness of the proposed RSSM algorithm. Moreover, with a uniform \tilde{p}_t , the proposed RSSM achieves the lowest KL divergence to true data samples in the three loss functions.

Moreover, the Langevin dynamics samples in Figure 2(e) show that even with the true score function, Langevin dynamics can not correctly recover the mixing coefficient in finite steps (20 steps in this case), demonstrating the slow mixing problem and further verifying the necessity of diffusion models even with given energy or score functions.

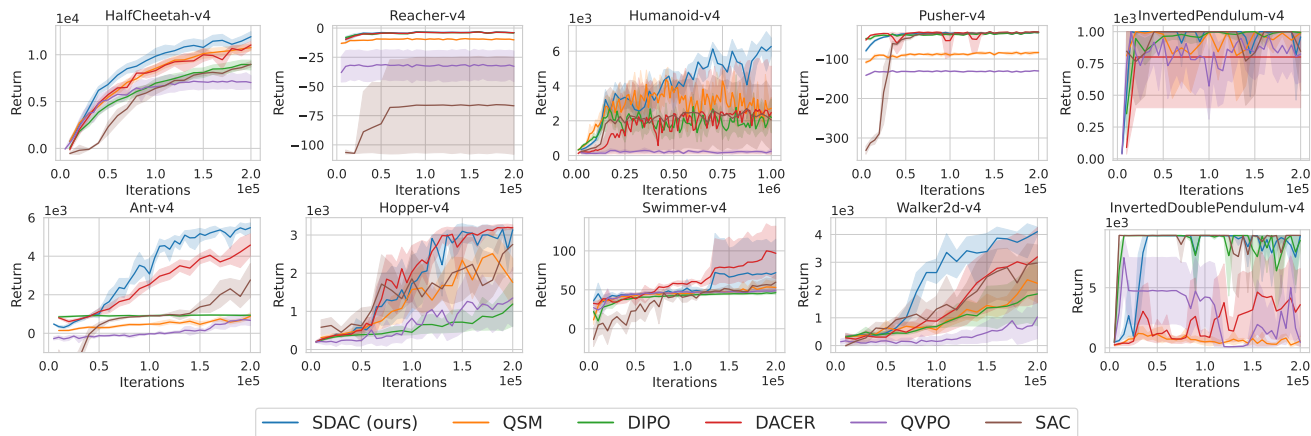


Figure 3: Average return over 20 evaluation episodes every 25k iterations (125k for Humanoid) during training. We select the top 5 baselines ranked by average performance over all tasks for clarity. The errorbars are standard deviations over 5 random seeds.

5.2 OpenAI Gym MuJoCo Tasks

5.2.1 Experimental Setup

We implemented our algorithm with the JAX package³ and evaluated the performance on 10 OpenAI Gym MuJoCo v4 tasks. All environments except Humanoid-v4 are trained over 200K iterations with a total of 1 million environment interactions while Humanoid-v4 has five times more.

Baselines. The baselines include two families of model-free RL algorithms. The first family is diffusion

³The implementation will be published upon acceptance.

policy RL, which includes a collection of recent diffusion-policy online RLs including QSM Psenka et al. (2023), QVPO Ding et al. (2024a), DACER Wang et al. (2024), DIPO Yang et al. (2023) and DPPO Ren et al. (2024). The second family is classic model-free online RL baselines including PPO Schulman et al. (2017), TD3 Fujimoto et al. (2018) and SAC Haarnoja et al. (2018a). A more detailed explanation to the baselines can be found in Appendix C.2.

5.2.2 Experimental Results

The performance and training curves are shown in Table 1 and Figure 3, which shows that our proposed algorithm outperforms all the baselines in all OpenAI Gym MuJoCo environments except Swimmer. Especially, for those complex locomotion tasks including the HalfCheetah, Walker2d, Ant, and Humanoid, we obtained **32.8%**, **35.0%**, **127.3%**, **143.5%** performance improvement compared to SAC and **at least 6.4%**, **36.7%**, **32.1%**, **23.1%** performance improvement compared to other diffusion-policy online RL baselines (not the same for all environments), respectively, demonstrating the superior and consistent performance of our proposed algorithm and the true potential of diffusion policies in online RL.

Moreover, the performance of the proposed SDAC is very stable and consistently good for all the tasks, demonstrating the superior robustness of SDAC. On the contrary, every diffusion-policy RL baseline performed badly on one or some tasks. For example, QSM failed the InvertedDoublePendulum, possibly because its true value function is known to be highly non-smooth. The non-smooth nature results in bad score function estimations since QSM matches the score function by differentiating the Q -functions. QVPO failed Reacher and Pusher since it cannot handle negative Q -functions. DACER failed InvertedPendulum despite its good performance in some complex tasks, probably due to the gradient instability when backpropagated recursively.

Computation and memory cost. We count the GPU memory allocations and total computation time listed in Table 2. The computation is conducted on a desktop with AMD Ryzen 9 7950X CPU, 96 GB memory, and NVIDIA RTX 4090 GPU. We achieve low memory consumption and faster computations compared to other diffusion-policy baselines. Note that the QSM essentially conducts the Langevin dynamics, which does not involve diffusion policies with the multi-level noise perturbation in essence. We can still achieve a comparable computation time and memory cost with QSM, indicating the proposed SDAC does not add much extra computational cost due to the diffusion policies.

Table 2: GPU memory allocation and total compute time of 200K iterations and 1 million environment interactions. *QSM did not learn diffusion policies essentially thus the computation is lightweight.

Algorithm	GPU Memory (MB)	Training time (min)
QSM*	997	14.23
QVPO	5219	30.90
DACER	1371	27.61
DIPO	5096	19.31
DPPO	1557	95.16
SDAC (ours)	1113	16.10

Sensitivity analysis. In Figure 4, we perform sensitivity analyses of different diffusion steps and diffusion noise schedules. Results show that 10 and 20 diffusion steps obtain comparable results, both outperforming the 30-step setting. The linear and cosine noise schedules perform similarly, and both outperform the variance preserve schedule. Therefore we choose 20 steps and cosine schedules for all tasks. The results also shows that SDAC is robust to diffusion process hyperparameters.

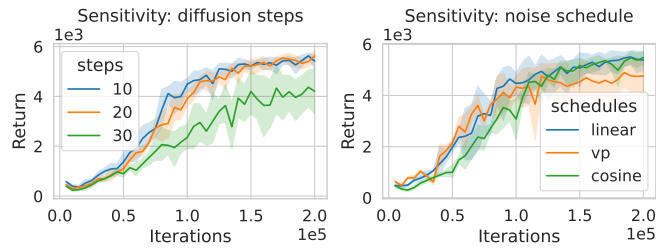


Figure 4: Sensitivity analysis on diffusion steps and diffusion noise schedule on Ant-v4.

6 Conclusion

In this paper, we proposed Soft Diffusion Actor-Critic (SDAC), an efficient diffusion policy training algorithm tailored for online RL. Regarding diffusion models as noise-perturbed EBMs, we develop the reverse sampling score matching to train diffusion models with access only to the energy functions and bypass sampling from the data distribution. In this way, we can train a diffusion policy with only access to the soft Q -function as the energy functions in online maximum entropy RL. Empirical results have shown superior performance compared to SAC and other recent diffusion policy online RLs. Possible future directions include improving the stability of diffusion policies and efficient exploration scheme design.

References

- Chen, H., Lu, C., Ying, C., Su, H., and Zhu, J. Offline reinforcement learning via high-fidelity generative behavior modeling. *arXiv preprint arXiv:2209.14548*, 2022.
- Chi, C., Xu, Z., Feng, S., Cousineau, E., Du, Y., Burchfiel, B., Tedrake, R., and Song, S. Diffusion policy: Visuomotor policy learning via action diffusion. *The International Journal of Robotics Research*, pp. 02783649241273668, 2023.
- Ding, S., Hu, K., Zhang, Z., Ren, K., Zhang, W., Yu, J., Wang, J., and Shi, Y. Diffusion-based reinforcement learning via q-weighted variational policy optimization. *arXiv preprint arXiv:2405.16173*, 2024a.
- Ding, Z., Zhang, A., Tian, Y., and Zheng, Q. Diffusion world model: Future modeling beyond step-by-step rollout for offline reinforcement learning. *arXiv preprint arXiv:2402.03570*, 2024b.
- Du, Y., Yang, S., Dai, B., Dai, H., Nachum, O., Tenenbaum, J., Schuurmans, D., and Abbeel, P. Learning universal policies via text-guided video generation. *Advances in Neural Information Processing Systems*, 36, 2024.
- Fujimoto, S., Hoof, H., and Meger, D. Addressing function approximation error in actor-critic methods. In *International conference on machine learning*, pp. 1587–1596. PMLR, 2018.
- Haarnoja, T., Tang, H., Abbeel, P., and Levine, S. Reinforcement Learning with Deep Energy-Based Policies, July 2017.
- Haarnoja, T., Zhou, A., Abbeel, P., and Levine, S. Soft actor-critic: Off-policy maximum entropy deep reinforcement learning with a stochastic actor. In *International conference on machine learning*, pp. 1861–1870. PMLR, 2018a.
- Haarnoja, T., Zhou, A., Hartikainen, K., Tucker, G., Ha, S., Tan, J., Kumar, V., Zhu, H., Gupta, A., Abbeel, P., et al. Soft actor-critic algorithms and applications. *arXiv preprint arXiv:1812.05905*, 2018b.
- Hansen-Estruch, P., Kostrikov, I., Janner, M., Kuba, J. G., and Levine, S. Idql: Implicit q-learning as an

- actor-critic method with diffusion policies. *arXiv preprint arXiv:2304.10573*, 2023.
- Ho, J., Jain, A., and Abbeel, P. Denoising Diffusion Probabilistic Models. In *Advances in Neural Information Processing Systems*, volume 33, pp. 6840–6851. Curran Associates, Inc., 2020.
- Huang, X., Chi, Y., Wang, R., Li, Z., Peng, X. B., Shao, S., Nikolic, B., and Sreenath, K. Diffuseloco: Real-time legged locomotion control with diffusion from offline datasets. *arXiv preprint arXiv:2404.19264*, 2024.
- Jain, V., Akhound-Sadegh, T., and Ravanbakhsh, S. Sampling from energy-based policies using diffusion. *arXiv preprint arXiv:2410.01312*, 2024.
- Janner, M., Du, Y., Tenenbaum, J. B., and Levine, S. Planning with diffusion for flexible behavior synthesis. *arXiv preprint arXiv:2205.09991*, 2022.
- Karras, T., Aittala, M., Aila, T., and Laine, S. Elucidating the Design Space of Diffusion-Based Generative Models, October 2022.
- Ke, T.-W., Gkanatsios, N., and Fragkiadaki, K. 3d diffuser actor: Policy diffusion with 3d scene representations. *arXiv preprint arXiv:2402.10885*, 2024.
- Parisi, G. Correlation functions and computer simulations. *Nuclear Physics B*, 180(3):378–384, 1981.
- Psenka, M., Escontrela, A., Abbeel, P., and Ma, Y. Learning a diffusion model policy from rewards via q-score matching. *arXiv preprint arXiv:2312.11752*, 2023.
- Puterman, M. L. *Markov decision processes: discrete stochastic dynamic programming*. John Wiley & Sons, 2014.
- Ramesh, A., Pavlov, M., Goh, G., Gray, S., Voss, C., Radford, A., Chen, M., and Sutskever, I. Zero-shot text-to-image generation. In *International conference on machine learning*, pp. 8821–8831. Pmlr, 2021.
- Ren, A. Z., Lidard, J., Ankile, L. L., Simeonov, A., Agrawal, P., Majumdar, A., Burchfiel, B., Dai, H., and Simchowitz, M. Diffusion policy optimization. *arXiv preprint arXiv:2409.00588*, 2024.
- Rigter, M., Yamada, J., and Posner, I. World models via policy-guided trajectory diffusion. *arXiv preprint arXiv:2312.08533*, 2023.
- Saharia, C., Chan, W., Saxena, S., Li, L., Whang, J., Denton, E. L., Ghasemipour, K., Gontijo Lopes, R., Karagol Ayan, B., Salimans, T., et al. Photorealistic text-to-image diffusion models with deep language understanding. *Advances in neural information processing systems*, 35:36479–36494, 2022.
- Scheikl, P. M., Schreiber, N., Haas, C., Freymuth, N., Neumann, G., Lioutikov, R., and Mathis-Ullrich, F. Movement primitive diffusion: Learning gentle robotic manipulation of deformable objects. *IEEE Robotics and Automation Letters*, 2024.
- Schulman, J., Wolski, F., Dhariwal, P., Radford, A., and Klimov, O. Proximal policy optimization algorithms. *arXiv preprint arXiv:1707.06347*, 2017.
- Shribak, D., Gao, C.-X., Li, Y., Xiao, C., and Dai, B. Diffusion spectral representation for reinforcement learning. *arXiv preprint arXiv:2406.16121*, 2024.
- Sohl-Dickstein, J., Weiss, E., Maheswaranathan, N., and Ganguli, S. Deep Unsupervised Learning using Nonequilibrium Thermodynamics. In *Proceedings of the 32nd International Conference on Machine*

- Learning*, pp. 2256–2265. PMLR, June 2015.
- Song, J., Meng, C., and Ermon, S. Denoising Diffusion Implicit Models, October 2022.
- Song, Y. and Ermon, S. Generative modeling by estimating gradients of the data distribution. *Advances in neural information processing systems*, 32, 2019.
- Song, Y. and Kingma, D. P. How to train your energy-based models. *arXiv preprint arXiv:2101.03288*, 2021.
- Song, Y., Sohl-Dickstein, J., Kingma, D. P., Kumar, A., Ermon, S., and Poole, B. Score-Based Generative Modeling through Stochastic Differential Equations, February 2021.
- Vincent, P. A Connection Between Score Matching and Denoising Autoencoders. *Neural Computation*, 23 (7):1661–1674, July 2011. ISSN 0899-7667, 1530-888X. doi: 10.1162/NECO_a.00142.
- Wang, Y., Wang, L., Jiang, Y., Zou, W., Liu, T., Song, X., Wang, W., Xiao, L., Wu, J., Duan, J., and Li, S. E. Diffusion Actor-Critic with Entropy Regulator, December 2024.
- Wang, Z., Hunt, J. J., and Zhou, M. Diffusion policies as an expressive policy class for offline reinforcement learning. *arXiv preprint arXiv:2208.06193*, 2022.
- Yang, L., Huang, Z., Lei, F., Zhong, Y., Yang, Y., Fang, C., Wen, S., Zhou, B., and Lin, Z. Policy representation via diffusion probability model for reinforcement learning. *arXiv preprint arXiv:2305.13122*, 2023.

A Related works

Diffusion models for decision making. Due to their rich expressiveness in modeling complex and multimodal distributions, diffusion models have been leveraged to represent stochastic policies Wang et al. (2022); Chen et al. (2022); Hansen-Estruch et al. (2023), plan trajectories Janner et al. (2022); Chi et al. (2023); Du et al. (2024) and capture transition dynamics Rigter et al. (2023); Ding et al. (2024b); Shribak et al. (2024). Specifically, we focus on the diffusion policies. Diffusion policies have been primarily used on offline RL with expert datasets, where the denoising score matching (5) is still available and the learned Q -function only provides extra guidance such as regularization Wang et al. (2022) or multiplication in the energy function. However, in online RL we do not have the dataset, thus denoising score matching is impossible.

Diffusion Models. Diffusion models have a dual interpretation of EBMs and latent variable models. The latent variable interpretation is motivated by the solving reverse-time diffusion thermodynamics via multiple layers of decoder networks Sohl-Dickstein et al. (2015). It was later refined by Ho et al. (2020) via simplified training loss. The EBM interpretation aims to solve pitfalls in Langevin dynamics sampling by adding progressively decreasing noise Song & Ermon (2019). Then the two viewpoints are merged together with viewpoints from stochastic differential equations Song et al. (2021), followed by numerous improvements on the training and sampling design Song et al. (2022); Karras et al. (2022).

Noise-conditioned score networks. A equivalent approaches developed by Song & Ermon (2019) simultaneously with diffusion models is to fit the score function of a series of noise-perturbed data distribution $\mathcal{N}(\mathbf{x}_i; \mathbf{x}, \sigma_i^2 \mathbf{I})$, $i = \{1, 2, \dots, K\}$ with a noise schedule $\sigma_1 > \sigma_2 > \dots > \sigma_K$. The resulting models, named the noise-conditioned score networks (NCSN) $f_\theta(\mathbf{x}_i; \sigma_i)$, take the noise level into the inputs and are learned by denoising score matching Vincent (2011)

$$\mathbb{E}_{\mathbf{x} \sim p, \mathbf{x}_i \sim \mathcal{N}(\mathbf{x}, \sigma_i^2 \mathbf{I})} [\|f_\theta(\mathbf{x}_i; \sigma_i) - \nabla_{\mathbf{x}_i} \log q(\mathbf{x}_i | \mathbf{x})\|^2] \quad (18)$$

Then in the sampling stage, Song & Ermon (2019) uses the Langevin dynamics $\mathbf{x}_{i+1} = \mathbf{x}_i + \eta \nabla_{\mathbf{x}_i} \log q(\mathbf{x}_i | \mathbf{x}) + \sqrt{2\eta} \mathbf{z}_i$ to sample from energy function. Song & Ermon (2019) additionally replace the original score function $\nabla_{\mathbf{x}_i} \log q(\mathbf{x}_i | \mathbf{x})$ in the Langevin dynamics with the learned noisy score function $f_\theta(\tilde{\mathbf{x}}; \sigma_i)$:

$$\mathbf{x}_{i+1} \leftarrow \mathbf{x}_i + \eta f_\theta(\tilde{\mathbf{x}}; \sigma_i) + \sqrt{2\eta} \mathbf{z}_i, \quad i = 0, \dots, K \quad (19)$$

named as annealed Langevin dynamics. The scheduled noise perturbation design significantly improved the image generation performance to match the state-of-the-art (SOTA) at that time Song & Ermon (2019), which is further refined by DDPM.

We can see that the annealed Langevin dynamics (19) resembles the DDPM sampling (6) with different scale factors, and the denoising score matching loss (18) is equivalent to (5). Therefore, DDPM can be interpreted as EBMs with multi-level noise perturbations. A more thorough discussion on their equivalency can also be found in Ho et al. (2020); Song et al. (2021).

B Derivations

B.1 Derivations of Proposition 3.1

We repeat Proposition 3.1 here,

Proposition 3.1 (Diffusion models as noise-perturbed EBMs). *The score network $s_\theta(\mathbf{a}_t; \mathbf{s}, t)$ in (5) matches noise-perturbed score functions, $\nabla_{\mathbf{a}_t} \log \tilde{\pi}_t(\mathbf{a}_t | \mathbf{s})$, where state \mathbf{s} is added to inputs of score network $s_\theta(\mathbf{a}_t; \mathbf{s}, t)$ to handle conditional distributions, $p_0(\cdot)$ in (5) refers to $\pi_{\text{target}}(\cdot | \mathbf{s})$ in the policy learning setting.*

Proof. This can be shown by checking the gradient estimator of $\nabla_{\mathbf{a}_t} \log \tilde{\pi}_t(\mathbf{a}_t|\mathbf{s}_t)$, i.e.,

$$\begin{aligned}\nabla_{\mathbf{a}_t} \log \tilde{\pi}_t(\mathbf{a}_t|\mathbf{s}_t) &= \frac{\nabla_{\mathbf{a}_t} \tilde{\pi}_t(\mathbf{a}_t|\mathbf{s})}{\tilde{\pi}_t(\mathbf{a}_t|\mathbf{s})} = \frac{\nabla_{\mathbf{a}_t} \int q_{t|0}(\mathbf{a}_t|\mathbf{a}_0) \pi_{\text{target}}(\mathbf{a}_0|\mathbf{s}) d\mathbf{a}_0}{\tilde{\pi}_t(\mathbf{a}_t|\mathbf{s})} \\ &= \int \nabla_{\mathbf{a}_t} \log q_{t|0}(\mathbf{a}_t|\mathbf{a}_0) \underbrace{\frac{q_{t|0}(\mathbf{a}_t|\mathbf{a}_0) \pi_{\text{target}}(\mathbf{a}_0|\mathbf{s})}{\tilde{\pi}_t(\mathbf{a}_t|\mathbf{s})}}_{p_{0|t}(\mathbf{a}_0|\mathbf{a}_t, \mathbf{s})} d\mathbf{a}_0\end{aligned}$$

We match the noise-perturbed score function via a neural network $s_\theta(\mathbf{a}_t; \mathbf{s}, t)$ via optimizing the expectation of square error over $\mathbf{a}_t \sim \tilde{\pi}_t(\cdot|\mathbf{s})$,

$$\begin{aligned}& \mathbb{E}_{\mathbf{a}_t \sim \tilde{\pi}_t} \left[\|s_\theta(\mathbf{a}_t; \mathbf{s}, t) - \nabla_{\mathbf{a}_t} \log \tilde{\pi}_t(\mathbf{a}_t|\mathbf{s})\|^2 \right] \\ &= \mathbb{E}_{\mathbf{a}_t \sim \tilde{\pi}_t} \left[\left\| s_\theta(\mathbf{a}_t; \mathbf{s}, t) - \int \nabla_{\mathbf{a}_t} \log q_{t|0}(\mathbf{a}_t|\mathbf{a}_0) \frac{q_{t|0}(\mathbf{a}_t|\mathbf{a}_0) \pi_{\text{target}}(\mathbf{a}_0|\mathbf{s})}{\tilde{\pi}_t(\mathbf{a}_t|\mathbf{s})} d\mathbf{a}_0 \right\|^2 \right] \\ &= \mathbb{E}_{\mathbf{a}_t \sim \tilde{\pi}_t} \left[\|s_\theta(\mathbf{a}_t; \mathbf{s}, t)\|^2 \right] - 2 \mathbb{E}_{\mathbf{a}_t \sim \tilde{\pi}_t} \left[\left\langle s_\theta(\mathbf{a}_t; \mathbf{s}, t), \int \nabla_{\mathbf{a}_t} \log q_{t|0}(\mathbf{a}_t|\mathbf{a}_0) \frac{q_{t|0}(\mathbf{a}_t|\mathbf{a}_0) \pi_{\text{target}}(\mathbf{a}_0|\mathbf{s})}{\tilde{\pi}_t(\mathbf{a}_t|\mathbf{s})} d\mathbf{a}_0 \right\rangle \right] + \text{constant}\end{aligned}\tag{20}$$

$$= \mathbb{E}_{\mathbf{a}_t \sim \tilde{\pi}_t} \left[\|s_\theta(\mathbf{a}_t; \mathbf{s}, t)\|^2 \right] - 2 \iint \left\langle s_\theta(\mathbf{a}_t; \mathbf{s}, t), \tilde{\pi}_t(\mathbf{a}_t|\mathbf{s}) \nabla_{\mathbf{a}_t} \log q_{t|0}(\mathbf{a}_t|\mathbf{a}_0) \frac{q_{t|0}(\mathbf{a}_t|\mathbf{a}_0) \pi_{\text{target}}(\mathbf{a}_0|\mathbf{s})}{\tilde{\pi}_t(\mathbf{a}_t|\mathbf{s})} \right\rangle d\mathbf{a}_0 d\mathbf{a}_t + \text{constant}\tag{21}$$

$$= \mathbb{E}_{\mathbf{a}_t \sim \tilde{\pi}_t} \left[\|s_\theta(\mathbf{a}_t; \mathbf{s}, t)\|^2 \right] - 2 \mathbb{E}_{\mathbf{a}_0 \sim \pi_{\text{target}}, \mathbf{a}_t \sim q_{t|0}} \left[\langle s_\theta(\mathbf{a}_t; \mathbf{s}, t), \nabla_{\mathbf{a}_t} \log q_{t|0}(\mathbf{a}_t|\mathbf{a}_0) \rangle \right] + \text{constant}\tag{22}$$

$$= \mathbb{E}_{\substack{\mathbf{a}_0 \sim \pi_{\text{target}} \\ \mathbf{a}_t \sim q_{t|0}}} \left[\|s_\theta(\mathbf{a}_t; \mathbf{s}, t) - \nabla_{\mathbf{a}_t} \log q_{t|0}(\mathbf{a}_t|\mathbf{a}_0)\|^2 \right] + \text{constant}\tag{23}$$

where the **constant** denotes constants that are irrelevant with θ . Therefore, minimizing the difference between $s_\theta(\mathbf{a}_t; \mathbf{s}, t)$ and $\nabla_{\mathbf{a}_t} \log \tilde{\pi}_t(\mathbf{a}_t|\mathbf{s})$ also implies minimizing the difference between $s_\theta(\mathbf{a}_t; \mathbf{s}, t)$ and $\nabla_{\mathbf{a}_t} \log q_{t|0}(\mathbf{a}_t|\mathbf{a}_0)$. This concludes the proof of Proposition 3.1. \square

B.2 Derivations of Theorem 3.2

Theorem 3.2 shows that we can match the score network $s_\theta(\mathbf{a}_t; \mathbf{s}, t)$ with noise-perturbed policy score function $\nabla_{\mathbf{a}_t} \log \tilde{\pi}_t(\mathbf{a}_t|\mathbf{s})$ without sampling from π_{target} like denoising score matching (5). Let us restate Theorem 3.2 and provide the proof below.

Theorem 3.2 (Reverse sampling score matching (RSSM)). *Define $\tilde{p}_t(\cdot|\mathbf{s})$ as a sampling distribution whose support contains the support of $\tilde{\pi}_t(\cdot|\mathbf{s})$ given \mathbf{s} . Then we can learn the score network $s_\theta(\mathbf{a}_t; \mathbf{s}, t)$ to match with the score function of noise-perturbed policy $\nabla_{\mathbf{a}_t} \log \tilde{\pi}_t(\mathbf{a}_t|\mathbf{s})$ via minimizing*

$$\mathbb{E}_{\substack{\mathbf{a}_t \sim \tilde{p}_t \\ \tilde{\mathbf{a}}_0 \sim \tilde{q}_{0|t}}} \left[\exp(Q(\mathbf{s}, \tilde{\mathbf{a}}_0)/\lambda) \|s_\theta(\mathbf{a}_t; \mathbf{s}, t) - \nabla_{\tilde{\mathbf{a}}_0} \tilde{q}_{0|t}(\tilde{\mathbf{a}}_0|\mathbf{a}_t)\|^2 \right]\tag{9}$$

where we abbreviate $Q^{\pi_{\text{old}}}$ with Q for simplicity and $\tilde{q}_{0|t}$ is the **reverse sampling** distribution defined as

$$\tilde{q}_{0|t}(\tilde{\mathbf{a}}_0|\mathbf{a}_t) := \mathcal{N}\left(\mathbf{a}_0; \frac{1}{\sqrt{\bar{\alpha}_t}} \mathbf{a}_t, \frac{1 - \bar{\alpha}_t}{\bar{\alpha}_t} \mathbf{I}\right)\tag{10}$$

which means $\tilde{\mathbf{a}}_0 = \frac{1}{\sqrt{\bar{\alpha}_t}} \mathbf{a}_t - \sqrt{\frac{1 - \bar{\alpha}_t}{\bar{\alpha}_t}} \boldsymbol{\epsilon}$ for $\boldsymbol{\epsilon} \sim \mathcal{N}(0, \mathbf{I})$.

Proof. The proof sketch consists of two major steps, reformulating the noise-perturbed score function and applying the reverse sampling trick.

Reformatting the noise-perturbed score function. First, we slightly reformat derivations of the

noise-perturbed score function in Proposition 3.1 starting from (7),

$$\begin{aligned}
& \nabla_{\mathbf{a}_t} \log \tilde{\pi}_t(\mathbf{a}_t | \mathbf{s}) \\
&= \int \nabla_{\mathbf{a}_t} \log q_{t|0}(\mathbf{a}_t | \mathbf{a}_0) \frac{q_{t|0}(\mathbf{a}_t | \mathbf{a}_0) \pi_{\text{target}}(\mathbf{a}_0 | \mathbf{s})}{\tilde{\pi}_t(\mathbf{a}_t | \mathbf{s})} d\mathbf{a}_0 \\
&= \frac{\int \nabla_{\mathbf{a}_t} \log q_{t|0}(\mathbf{a}_t | \mathbf{a}_0) q_{t|0}(\mathbf{a}_t | \mathbf{a}_0) \exp(Q(\mathbf{s}, \mathbf{a}_0) / \lambda) d\mathbf{a}_0}{Z_t(\mathbf{a}_t; \mathbf{s})}
\end{aligned} \tag{24}$$

where the second equality holds since we multiply both the denominator and numerator with normalization constant $\int \exp(Q(\mathbf{s}, \mathbf{a}_0) / \lambda) d\mathbf{a}_0$ with:

$$Z_t(\mathbf{a}_t; \mathbf{s}) := \tilde{\pi}_t(\mathbf{a}_t | \mathbf{s}) \int \exp(Q(\mathbf{s}, \mathbf{a}_0) / \lambda) d\mathbf{a}_0 \tag{25}$$

$$= \int \frac{\exp(Q(\mathbf{s}, \mathbf{a}_0) / \lambda)}{\int \exp(Q(\mathbf{s}, \mathbf{a}_0) / \lambda) d\mathbf{a}_0} q_{t|0}(\mathbf{a}_t | \mathbf{a}_0) d\mathbf{a}_0 \int \exp(Q(\mathbf{s}, \mathbf{a}_0) / \lambda) d\mathbf{a}_0 \tag{26}$$

$$= \int \exp(Q(\mathbf{s}, \mathbf{a}_0) / \lambda) q_{t|0}(\mathbf{a}_t | \mathbf{a}_0) d\mathbf{a}_0 \tag{27}$$

We use the score network s_θ to learn (24) via minimizing the square error, resulting the following loss term given \mathbf{a}_t ,

$$\begin{aligned}
& \|s_\theta(\mathbf{a}_t, \mathbf{s}, t) - \nabla_{\mathbf{a}_t} \log \tilde{\pi}_t(\mathbf{a}_t | \mathbf{s})\|^2 \\
&= \left\| s_\theta(\mathbf{a}_t, \mathbf{s}, t) - \frac{\int \nabla_{\mathbf{a}_t} \log q_{t|0}(\mathbf{a}_t | \mathbf{a}_0) q_{t|0}(\mathbf{a}_t | \mathbf{a}_0) \exp(Q(\mathbf{s}, \mathbf{a}_0) / \lambda) d\mathbf{a}_0}{Z_t(\mathbf{a}_t; \mathbf{s})} \right\|^2 \\
&= \frac{1}{Z(\mathbf{a}_t; \mathbf{s})} \|s_\theta(\mathbf{a}_t, \mathbf{s}, t)\|^2 \underbrace{\left(\int \exp(Q(\mathbf{s}, \mathbf{a}_0) / \lambda) q_{t|0}(\mathbf{a}_t | \mathbf{a}_0) d\mathbf{a}_0 \right)}_{Z(\mathbf{a}_t; \mathbf{s})} \\
&\quad - \frac{2}{Z(\mathbf{a}_t; \mathbf{s})} \left\langle s_\theta(\mathbf{a}_t, \mathbf{s}, t), \int \nabla_{\mathbf{a}_t} \log q_{t|0}(\mathbf{a}_t | \mathbf{a}_0) q_{t|0}(\mathbf{a}_t | \mathbf{a}_0) \exp(Q(\mathbf{s}, \mathbf{a}_0) / \lambda) d\mathbf{a}_0 \right\rangle + \text{constant} \tag{28}
\end{aligned}$$

$$\begin{aligned}
&= \int \frac{1}{Z(\mathbf{a}_t; \mathbf{s})} q_{t|0}(\mathbf{a}_t | \mathbf{a}_0) \left(\exp(Q(\mathbf{s}, \mathbf{a}_0) / \lambda) \left(\|s_\theta(\mathbf{a}_t, \mathbf{s}, t)\|^2 - 2 \langle s_\theta(\mathbf{a}_t, \mathbf{s}, t), \nabla_{\mathbf{a}_t} \log q_{t|0}(\mathbf{a}_t | \mathbf{a}_0) \rangle \right) \right) d\mathbf{a}_0 + \text{constant} \\
&= \int \frac{1}{Z(\mathbf{a}_t; \mathbf{s})} q_{t|0}(\mathbf{a}_t | \mathbf{a}_0) \left(\exp(Q(\mathbf{s}, \mathbf{a}_0) / \lambda) \|s_\theta(\mathbf{a}_t, \mathbf{s}, t) - \nabla_{\mathbf{a}_t} \log q_{t|0}(\mathbf{a}_t | \mathbf{a}_0)\|^2 \right) d\mathbf{a}_0 + \text{constant} \tag{29}
\end{aligned}$$

where we abbreviate the constants that are irrelevant to θ in the calculation.

Weight function g . For more rigorous derivations, we denote a weight function $g : \mathcal{A} \times \mathcal{S} \rightarrow \mathbb{R}^+$ constructed by

$$g(\mathbf{a}_t; \mathbf{s}) = Z(\mathbf{a}_t; \mathbf{s}) \tilde{p}(\mathbf{a}_t | \mathbf{s}) \tag{30}$$

As $Z(\mathbf{a}_t; \mathbf{s})$ is $\tilde{\pi}_t$ scaled by normalization constant $\int \exp(Q(\mathbf{s}, \mathbf{a}_0)) d\mathbf{a}_0$ and the support of $\tilde{p}(\cdot | \mathbf{s})$ contains $\tilde{\pi}_t(\cdot | \mathbf{s})$, we know that $g(\mathbf{a}_t; \mathbf{s})$ is strictly positive on the support of $\tilde{\pi}(\cdot | \mathbf{s})$. Therefore, we can optimize the squared error over \mathbf{a}_t via the

$$\begin{aligned}
\mathcal{L}^g(\theta; \mathbf{s}, t) &:= \int g(\mathbf{a}_t; \mathbf{s}) \|s_\theta(\mathbf{a}_t, t) - \nabla_{\mathbf{a}_t} \log \tilde{\pi}_t(\mathbf{a}_t | \mathbf{s})\|^2 d\mathbf{a}_t \\
&= \iint \frac{g(\mathbf{a}_t; \mathbf{s})}{Z(\mathbf{a}_t; \mathbf{s})} q_{t|0}(\mathbf{a}_t | \mathbf{a}_0) \left(\exp(Q(\mathbf{s}, \mathbf{a}_0) / \lambda) \|s_\theta(\mathbf{a}_t, \mathbf{s}, t) - \nabla_{\mathbf{x}_t} \log q_{t|0}(\mathbf{a}_t | \mathbf{a}_0)\|^2 \right) d\mathbf{a}_0 d\mathbf{a}_t + \text{constant} \\
&= \iint \tilde{p}(\mathbf{a}_t | \mathbf{s}) q_{t|0}(\mathbf{a}_t | \mathbf{a}_0) \left(\exp(Q(\mathbf{s}, \mathbf{a}_0) / \lambda) \|s_\theta(\mathbf{a}_t, \mathbf{s}, t) - \nabla_{\mathbf{x}_t} \log q_{t|0}(\mathbf{a}_t | \mathbf{a}_0)\|^2 \right) d\mathbf{a}_0 d\mathbf{a}_t + \text{constant} \tag{31}
\end{aligned}$$

where the equalities come from the results in (29) and definition of g in (30).

Reverse sampling trick. Then we replace $q_{t|0}$ with a reverse sampling distribution $\tilde{q}_{0|t}$ that satisfies

$$\tilde{q}_{0|t}(\mathbf{a}_0 | \mathbf{a}_t) = \mathcal{N} \left(\mathbf{a}_0; \frac{1}{\sqrt{\bar{\alpha}_t}} \mathbf{a}_t, \frac{1 - \bar{\alpha}_t}{\bar{\alpha}_t} \mathbf{I} \right) \propto q_{t|0}(\mathbf{a}_t | \mathbf{a}_0) = \mathcal{N}(\mathbf{a}_t; \sqrt{\bar{\alpha}_t} \mathbf{a}_0, (1 - \bar{\alpha}_t) \mathbf{I}), \tag{32}$$

and thus

$$\nabla_{\mathbf{a}_t} \log q_{t|0}(\mathbf{a}_t | \mathbf{a}_0) = \nabla_{\mathbf{a}_t} \log \tilde{q}_{0|t}(\mathbf{a}_0 | \mathbf{a}_t) = -\frac{\mathbf{a}_t - \sqrt{\tilde{\alpha}_t} \mathbf{a}_0}{1 - \tilde{\alpha}_t} \quad (33)$$

Then we continue via replacing q with \tilde{q} in (29), resulting in (29) equals

$$\begin{aligned} \mathcal{L}^g(\theta; \mathbf{s}, t) &= \iint \tilde{p}_t(\mathbf{a}_t | \mathbf{s}) \tilde{q}_{0|t}(\tilde{\mathbf{a}}_0 | \mathbf{a}_t) \left(\exp(Q(\mathbf{s}, \mathbf{a}_0)/\lambda) \left\| s_\theta(\mathbf{a}_t, \mathbf{s}, t) - \nabla_{\mathbf{x}_t} \log \tilde{q}_{0|t}(\tilde{\mathbf{a}}_0 | \mathbf{a}_t) \right\|^2 \right) d\tilde{\mathbf{a}}_0 d\mathbf{a}_t + \text{constant} \\ &= \mathbb{E}_{\mathbf{a}_t \sim \tilde{p}_t, \tilde{\mathbf{a}}_0 \sim \tilde{q}_{0|t}} \left[\exp(Q(\mathbf{s}, \tilde{\mathbf{a}}_0)/\lambda) \left\| s_\theta(\mathbf{a}_t, \mathbf{s}, t) - \nabla_{\mathbf{x}_t} \log \tilde{q}_{0|t}(\tilde{\mathbf{a}}_0 | \mathbf{a}_t) \right\|^2 \right] + \text{constant} \end{aligned} \quad (34)$$

which concludes the proof of Theorem 3.2. \square

C Additional Experimental Setup

C.1 Training Setups for the Toy Example

Consider Gaussian mixture model with density function

$$p_0(\mathbf{x}) = 0.8 * \frac{1}{2\pi} \exp\left(-\frac{\|\mathbf{x} - [3; 3]\|^2}{2}\right) + 0.2 * \frac{1}{2\pi} \exp\left(-\frac{\|\mathbf{x} + [3; 3]\|^2}{2}\right) \quad (35)$$

where the RSSM optimizes

$$\mathbb{E}_{\substack{\mathbf{x}_t \sim \tilde{p} \\ \mathbf{x}_0 \sim \tilde{q}_{0|t}}} \left[p_0(\tilde{\mathbf{x}}_0) \left\| s_\theta(\mathbf{x}_t; t) - \nabla_{\mathbf{x}_t} \log \tilde{q}_{0|t}(\tilde{\mathbf{x}}_0 | \mathbf{x}_t) \right\|^2 \right] \quad (36)$$

for the Gaussian sampling, $\tilde{p}(\mathbf{x}_t) = \mathcal{N}(0, 4\mathbf{I})$ for all t and for uniform sampling, \tilde{p}_t is a uniform distribution from $[-6, 6]$ on both dimensions. The score network is trained via the hyperparameters listed in Table 3. The Langevin dynamics has direct access to the true score function $\nabla_{\mathbf{x}} \log p_0(\mathbf{x})$.

Table 3: Hyperparameters for the toy example.

Name	Value	Name	Value
Learning rate	3e-4	Diffusion noise schedule	linear
Diffusion steps	20	Diffusion noise schedule start	0.001
Hidden layers	2	Diffusion noise schedule end	0.999
Hidden layer neurons	128	Training batch size	1024
Activation Function	LeakyReLU	Training epoches	300

C.2 Baselines

We include two families of methods as our baselines. For the first family of methods, we select 5 online diffusion-policy RL algorithms: QSM Psenka et al. (2023), QVPO Ding et al. (2024a), DACER Wang et al. (2024), DIPO Yang et al. (2023) and DPPO Ren et al. (2024). We include both off-policy (QSM, QVPO, DACER, DIPO) and on-policy (DPPO) diffusion RL methods among this group of algorithms. QSM follows a similar idea with Remark 3.4 to use the Langevin dynamic with derivatives of learned Q -function as the score function. QVPO derives a Q -weighted variational objective for diffusion policy training, yet this objective cannot handle negative rewards properly. DACER directly backward the gradient through the reverse diffusion process and proposes a GMM entropy regulator to balance exploration and exploitation. DIPO utilizes a two-stage strategy, which maintains a large number of state-action particles updated by the gradient of the Q -function, and then fit the particles with a diffusion model. DPPO constructs a two-layer MDP with diffusion steps and environment steps, respectively, and then performs

Proximal Policy Optimization on the overall MDP. In our experiments, we use the training-from-scratch setting of DPPO to ensure consistency with other methods.

The second family of baselines includes 3 classic model-free RL methods: PPO [Schulman et al. \(2017\)](#), TD3 [Fujimoto et al. \(2018\)](#) and SAC [Haarnoja et al. \(2018a\)](#). For PPO, we set the replay buffer size as 4096 and use every collected sample 10 times for gradient update. Across all baselines, we collect samples from 5 parallel environments in a total of 1 million environment interactions and 200k epoches/iterations. The results are evaluated with the average return of 20 episodes across 5 random seeds.

C.3 Hyperparameters

Table 4: Hyperparameters

Name	Value
Critic learning rate	3e-4
Policy learning rate	3e-4, linear annealing to 3e-5
Diffusion steps	20
Diffusion noise schedules	Cosine
Policy network hidden layers	3
Policy network hidden neurons	256
Policy network activation	Mish
Value network hidden layers	3
Value network hidden neurons	256
Value network activation	Mish
replay buffer size (off-policy onoy)	1 million

where the Cosine noise schedule means $\beta_t = 1 - \frac{\bar{\alpha}_t}{\alpha_{t-1}}$ with $\bar{\alpha}_t = \frac{f(t)}{f(0)}$, $f(t) = \cos\left(\frac{t/T+s}{1+s} * \frac{\pi}{2}\right)^2$.